Briefs

Maximum Allowable Bulk Defect Density for Generation–Recombination Noise-Free Device Operation

Fan-Chi Hou, Gijs Bosman, and Mark E. Law

***Abstract*—Generation–recombination noise associated with bulk defect levels in silicon is modeled in a partial differential equation-based device simulator to study the maximum allowable defect density that guarantees generation-recombination (g–r) noise-free operation in the presence of hot-carrier effects and space-charge injection.**

***Index Terms*—Carrier trapping, semiconductor defects, semiconductor device noise.**

I. Introduction

Many defects that exist in semiconductor devices are often unintentional. Elements such as carbon, oxygen, and various metals may be introduced to the wafer during processing steps, and then become carrier trap centers that affect device performance and produce generation–recombination (g–r) noise. The g–r noise is due to the random fluctuations in the trapping and detrapping rates in the defect trap centers in the forbidden band gap. This in turn causes the current or the voltage, depending on the condition at the contact terminal, to fluctuate as well. The generation and recombination transition has generally been characterized by the Shockley–Read–Hall (SRH) model. In this model, each defect species is specified by its defect density, its carrier capture coefficients, and its energy position relative to either the conductance or valence band. The focus of this paper is to study the maximum allowable bulk defect density that guarantees g–r noise-free device operation under bias. Having this information may guide the decision on the need for incorporating defect reduction steps in a low noise device fabrication process for such regions as the extrinsic base and drain and source access regions that are known to be sensitive to bulk g–r noise components. Both the local g–r noise strength and the transfer Green's function, which couples the carrier fluctuations in each differential volume of the device to a specific contact, depend on bias. Simple analytical g–r noise models indicate that the g–r current noise spectral density of a resistor is proportional to I^2 in the ohmic regime, where I is the current through the device. For a p-n diode, the noise may vary as I^c with $1 \leq c \leq 2$ depending on the physical location of the g–r noise sources. As a consequence, increasing the bias across a device or device region will nearly always lift a g–r noise component out of the thermal noise background. In practice however, carrier heating and space-charge injection from adjacent regions will lead to field dependent carrier mobilities and position dependent carrier and trapped electron densities resulting in a change of the observed g–r noise signature of a defect center at higher bias. It is difficult to unravel the full physical noise picture analytically under these conditions [1]. We therefore expanded the capabilities of a semiconductor device simulator with g–r and velocity fluctuation noise models to study these effects.

Manuscript received July 16, 2002. This work was supported by the Semiconductor Research Corporation. The review of this brief was arranged by Editor M. J. Deen.

The authors are with the Department of Electrical and Computer Engineering, University of Florida, Gainesville, FL 32611 USA (email: bosman@ece.ufl.edu; law@tec.ufl.edu).

Digital Object Identifier 10.1109/TED.2002.804705

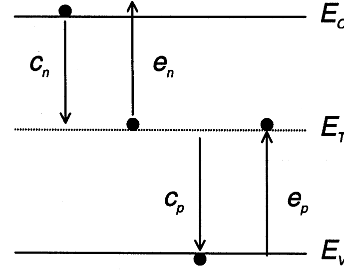

Fig. 1. Carrier transitions between the continuum states and localized defect states.

II. Implementation

The g–r process can be described by the SRH model, as shown in Fig. 1. For illustration purposes, assume there is one defect trap level in the band gap, and that the traps are acceptor-like. In addition to the three basic Shockley equations

$$F_\psi = -\frac{d^2\psi}{dr^2} - \frac{q}{\varepsilon}\left[p - n + N_D^+ - N_A^- - n_t\right] = 0 \quad (1)$$

$$F_n = \frac{dn}{dt} - \frac{1}{q}\nabla \cdot J_n - g_n + r_n - \gamma_n = 0 \quad (2)$$

$$F_p = \frac{dp}{dt} + \frac{1}{q}\nabla \cdot J_p - g_p + r_p + \gamma_p = 0 \quad (3)$$

a trapped electron continuity equation is added to the simulator to describe the carrier density fluctuations at the trap level E_t

$$F_{n_t} = \frac{dn_t}{dt} + g_n - r_n - g_p + r_p - \gamma_t = 0 \quad (4)$$

where γ_n, γ_p, and γ_t are the Langevin noise terms describing random transition rate fluctuations. The transition rates can be expressed for electrons as

$$r_n = c_n n\,(N_T - n_t) \quad \text{and} \quad g_n = c_n n_1 n_t \quad (5)$$

and for holes as

$$r_p = c_p p n_t \quad \text{and} \quad g_p = c_p p_1\,(N_T - n_t) \quad (6)$$

where N_T represents the defect density and n_1 and p_1 are the Shockley parameters.

The physics-based noise models are implemented into the device simulator using the impedance field method (IFM) [2]. Two elements are required to calculate the noise at the contact terminals. The first is the magnitude of the microscopic noise sources $K_{\gamma_\alpha,\gamma_\beta}$ (where $\alpha, \beta = n, p, n_t$) at each grid point. For the g–r noise process, the microscopic noise sources $K_{\gamma_\alpha,\gamma_\beta}$ are given by [3]

$$\begin{aligned} K_{\gamma_n,\gamma_n} &= 2g_n + 2r_n = -K_{\gamma_n,\gamma_t} \\ K_{\gamma_p,\gamma_p} &= 2g_p + 2r_p = -K_{\gamma_p,\gamma_t} \\ K_{\gamma_t,\gamma_t} &= K_{\gamma_n,\gamma_n} + K_{\gamma_p,\gamma_p}. \end{aligned} \quad (7)$$

The second element is the transfer Green's function that couples the perturbation of the PDEs from each grid point to the device terminals.

0018-9383/02$17.00 © 2002 IEEE

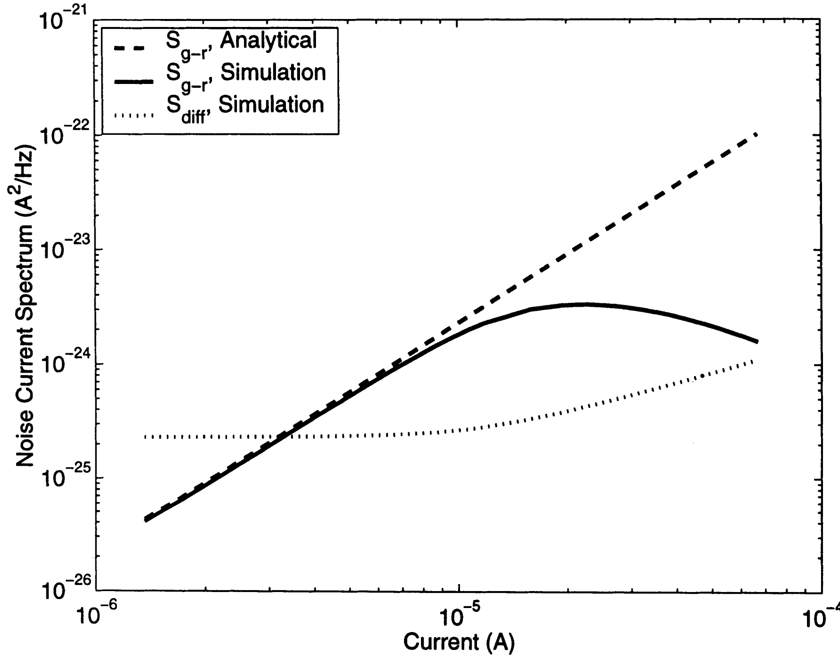

Fig. 2. Comparison between the simulated and analytical g–r current noise spectral density as a function of the bias voltage ($f = 1$ Hz). The dashed line represents expression (9). The solid line is the simulated g–r noise. The dotted line is the simulated velocity fluctuation noise.

The scalar Green's function $\tilde{G}$ for each carrier type at each node is obtained by perturbing the PDE associated with the carrier at the node, and then observing the changes at the contact terminals. The g–r noise voltage spectral density at an external contact terminal is calculated through the following expression [2]:

$$S_{V,gr} = \sum_{i=1}^{N_{\text{trap}}} \sum_{\alpha,\beta=n,p,n_t} \int_{vol} \tilde{G}_\alpha K_{\gamma_\alpha,\gamma_\beta} \tilde{G}_\beta^* dr \tag{8}$$

where N_{trap} is the number of trap levels in the device.

The g–r noise mechanism described above was implemented into FLorida Object-Oriented Device Simulator (FLOODS). FLOODS is a silicon, PDE-based, generalized box scheme device simulator using the drift-diffusion formalism augmented with field and doping dependent mobility models [4].

III. Simulation

To study and illustrate the effects of carrier heating and carrier injection on the g–r noise signature of bulk defects a two-dimensional n^+ -n-n^+ bulk silicon resistor was created. The n- and n^+-region are doped with $N_d = 10^{15}$ and $N_{d+} = 10^{18}$ cm^{-3} shallow donors, respectively, producing a room temperature Fermi-level at 0.265 eV below the conduction band in the center of the n-region. The length L of the n-region is 2 μm, and the n^+-regions are 0.5 μm long. The cross-sectional area A is 1 μm^2. A defect center at $E_T = E_C - 0.265$ eV, uniformly distributed, is chosen for the simulation. This choice was guided by the fact that trap levels close to E_F produce maximum local noise strengths [4] and thus represent a worst case scenario. Electron and hole capture coefficients c_n and c_p, and defect density N_T are set to 10^{-8} cm^3/s (typical values for neutral impurities) and, initially 10^{12} cm^{-3}. Since E_T is much closer to E_C than E_V, one can safely assume $g_n, r_n >> g_p, r_p$, $g_n \approx r_n$, and $c_n(n + n_1) >> c_p(p + p_1)$. With these assumptions, the analytical expression of the current noise spectral density of this structure at low frequencies and low bias becomes [5]

$$S_I(f \to 0) \approx \frac{4I^2}{LAn^2} \frac{n_1 n_t}{c_n (n + n_1)^2}. \tag{9}$$

Fig. 2 shows g–r noise simulations as a function of bias. Under low bias conditions, the g–r noise is below the velocity fluctuation noise and in good agreement with the analytical expression (9). When the bias increases, the magnitude of the simulated g–r noise emerges from the velocity fluctuation noise, reaches a peak and then starts to decrease due to predominantly space-charge injection. The injected electrons fill the traps and subsequently the g–r mechanism at that level becomes less effective due to a decrease in the recombination rate and, via detailed balance, generation rate. The result is then a decrease in the local g–r noise strength. In addition the simulation confirms that at low bias, where N is a constant, the Green's function is proportional to I. Under high bias conditions however, N increases with bias as the carrier injection into the n-region becomes significant and the Green's function becomes less bias dependent, reducing the coupling between local noise source and device terminal.

IV. Discussion

Fig. 2 shows that for the trap example selected the g–r noise dominates the velocity fluctuation noise over a wide bias range, hence the chosen trap density of 10^{12} cm^{-3} clearly exceeds the maximum allowable defect density $N_{T\max}$ for g–r noise-free operation of this example. The value of $N_{T\max}$ for this particular trap follows from equating the g–r noise magnitude with the magnitude of the velocity fluctuation noise component. Under low bias conditions in the ohmic regime, the quantity of $N_{T\max}$ can be derived analytically by setting (9) equal to $S_{I\Delta v} = 4kT/R$. Thus

$$N_{T\max} = \frac{kTL^2}{q\mu V^2} \frac{c_n (n + n_1)^3}{n_1}. \tag{10}$$

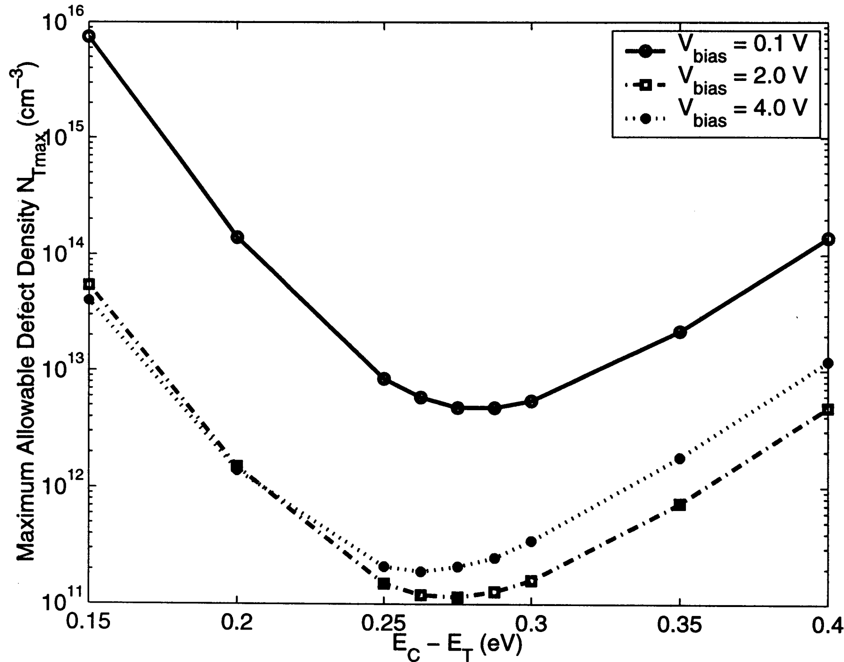

Fig. 3. $N_{T\max}$ plotted as a function of trap energy under different bias conditions.

Simulations were carried out by varying the value of N_T to obtain a g–r noise level equal to the velocity fluctuation noise level as a function of trap energy level for a bias of 0.1 V at room temperature with the c_n and c_p values previously specified. The simulation results are presented in Fig. 3 and agree with the low bias predictions of (10). The figure shows that defect levels close to the Fermi level at $E_C - E_F = 0.265$ eV require stricter constraints than defect levels further away from E_F, corroborating the fact that traps at the Fermi level produce g–r noise more effectively. Fig. 3 also shows that at higher bias lower defect densities are required for g–r noise-free operation primarily due to an increase in magnitude of the Green's function with bias. To estimate $N_{T\max}$ at high bias for a trap at the Fermi level, the worst case scenario, we use $n_1 = n$ and $n_t = 0.5N_T$.

The value of $S_{Igr}(0)$ of (9) needs to be compared with the magnitude of the velocity fluctuation noise $S_{I\Delta v}$ component as read from the simulated data presented in Fig. 2. Note that I, n, and $S_{I\Delta v}$ are affected by carrier heating and space-charge injection. The value of I follows from the simulated *I-V* characteristic, whereas n may be estimated from $n = N/(AL)$ with

$$N = \frac{CV}{q} + N_d AL \tag{11}$$

where $C = 1.7C_o$ with C_o representing the geometrical capacitance of the device. Equation (11) is based on early work by Lampert and Mark [6] and was later confirmed by Bosman *et al.* [7]. The value of $N_{T\max}$ can now be calculated as [5]

$$N_{T\max} = 2\frac{c_n N^3 S_{I\Delta v}(0)}{(ALI)^2} \tag{12}$$

resulting in $N_{T\max} = 1.4 \times 10^{11}$ cm^{-3} at 2 V and 2×10^{11} cm^{-3} at 4 V, respectively, in very good agreement with the simulated data presented in Fig. 3.

V. Conclusions

This study has shown that a PDE-based silicon device simulator augmented with Langevin noise sources is an accurate tool to determine the maximum allowable impurity density for g–r noise-free device operation in the presence of hot-carrier effects and space-charge injection.

References

[1] *Special Issue on Fluctuation Phenomena in Electronic and Photonic Devices, IEEE Trans. Electron Devices*, vol. 41, 1994.
[2] F. Bonani, G. Ghione, M. R. Pinto, and R. K. Smith, "An efficient approach to noise analysis through multidimensional physics-based models," *IEEE Trans. Electron Devices*, vol. 45, pp. 261–269, Jan. 1998.
[3] K. M. van Vliet, "Noise and admittance of the generation–recombination current involving SRH centers in the space-charge region of junction devices," *IEEE Trans. Electron Devices*, vol. ED-23, pp. 1236–1246, Nov. 1976.
[4] F.-C. Hou and G. Bosman, "Characterization of generation–recombination noise using a physics-based device noise simulator," in *Proc. 15th Int. Conf. Noise Phys. Syst. 1/f Fluct.*, C. Surya, Ed., London, U.K., 1999, pp. 35–38.
[5] F.-C. Hou, "Low-frequency bulk and surface generation–recombination noise simulations of semiconductor devices," Ph.D. dissertation, Univ. Florida, Gainesville, 2002.
[6] M. A. Lampert and P. Mark, *Current Injection in Solids*. New York: Academic, 1970.
[7] G. Bosman, R. J. J. Zijlstra, and F. Nava, "The longitudinal diffusion coefficient and mobility of hot electrons in silicon," *Solid State Electron.*, vol. 24, pp. 5–9, 1981.